CHEMISTRY OF MATERIALS

Article

pubs.acs.org/cm

Manifestation of the Difference in Reactivity of Silver Clusters in Contrast to Its Ions and Nanoparticles: The Growth of Metal Tipped Te Nanowires

Anirban Som,‡ A. K. Samal,‡ T. Udayabhaskararao, M. S. Bootharaju, and T. Pradeep*

DST Unit of Nanoscience (DST UNS) & Thematic Unit of Excellence (TUE), Department of Chemistry, Indian Institute of Technology Madras, Chennai, 600 036 Tamil Nadu, India

Supporting Information

ABSTRACT: Reactivity of two different nanosystems of silver, namely nanoparticles and atomically precise clusters, toward 1D tellurium nanowires (NWs) was probed and compared with the reaction of silver ions. While the reaction of nanoparticles and ions led to silver telluride nanowires, a different reactivity was exhibited by clusters which resulted in silver islands at different positions on the Te NWs. These hybrid Ag nodule-decorated Te NWs are sensitive to temperature, and they transform to dumbbell-shaped silver-tipped Te NWs upon solution phase annealing. Differences in chemical reactivity of nanoparticles of two different size regimes with nanowires are demonstrated. Synthetic methods of this kind will be useful in creating complex nanostructures which are difficult to be made in the solution phase.

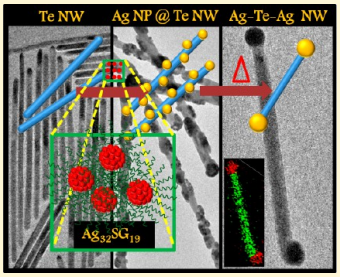

INTRODUCTION

Nanosystems have become enormously diverse in the past several years in terms of their chemical variety and structural attributes. However, the most common and widely researched nanosystems belong to zero- and one-dimensional categories.[1] While there have been many zero-dimensional particles belonging to metals, semiconductors and dielectrics, noble metal nanoparticles are the most widely researched systems. The most emerging category of zero dimensional noble metal nanosystems is their atomically precise analogues, called by a number of names such as quantum clusters (QCs),[2] nanoclusters,[3] superatoms,[4] or nanomolecules.[5] While gold nanoclusters have been extensively studied,[6,7] reports on their silver counterparts are limited.[8−10] Most of such studies are on synthesis,[11−15] characterization,[16−19] and properties,[20,21] while their chemistry is beginning to evolve.[22−27] They are typically labeled in terms of the number of atoms in the core such as Au_{25}, although the cluster is composed of ligands as well, protecting the core.

In the one-dimensional nanosystems, large chemical varieties have evolved in the past decade. Among these, tellurium, due to its inherent structural anisotropy, is prone to one-dimensional growth, and Te nanowires (NWs) of precise aspect ratio can be synthesized chemically.[28,29] Chemistry of these wires results in binary 1D systems,[30−33] and in special cases biphasic NWs[34−39] can also be synthesized. Properties of such systems with unusual morphological features have been rarely explored, although when done have led to intriguing applications.[38,40]

In this article, we introduce the chemistry of atomically precise clusters with 1D nanosystems, taking Ag QCs and Te NWs as reactants. As an example of Ag QCs, we have taken $Ag_{32}SG_{19}$ (SG refers to glutathione thiolate), a cluster reported by our group[41] as well as others.[42] The unprecedented and unique chemistry of these reactants lead to new nanosystems which have not been observed when the clusters were replaced with metal ions or nanoparticles (NPs). While the precise reasons for this unique chemistry are unknown, the observed structures, their reproducibility, and synthetic control this reaction offers, suggest new possibilities of nanochemistry. Extension of the reactivity to chemically similar systems and exploration of processes *in situ* would provide an insight into the chemistry between nanosystems.

EXPERIMENTAL SECTION

Chemicals. All the chemicals were commercially available and were used without further purification. Silver nitrate ($AgNO_3$, 99%) and glutathione (GSH, 97%) were purchased from SRL Chemical Co. Ltd., India. Sodium dodecyl sulfate (SDS, $C_{12}H_{25}O_4SNa$, 99%) was obtained from Acros. Tellurium dioxide (TeO_2, 99.9%) powder was purchased from Alfa Aesar. Hydrazine monohydrate ($N_2H_4{\cdot}H_2O$, 99−100%) was purchased from SD Fine Chemicals, India. Sodium borohydride ($NaBH_4$, 99.99%, Aldrich), ethanol (HPLC grade, 99.9%, Aldrich), and methanol (HPLC grade) were used as received.

Synthesis of $Ag_{32}SG_{19}$. Synthesis followed a method reported previously.[41] About 23 mg of $AgNO_3$(s) was added to 200 mg of GSH(s) at room temperature, and the mixture was ground well in a mortar to make Ag(I)SG. About 25 mg of $NaBH_4$(s) was added, and grinding was continued further for 10 more minutes. After that, 10 mL of distilled water was added slowly (in one mL step) which resulted in the formation of a reddish brown solution. Clusters were then precipitated immediately by the addition of excess ethanol. The resulting precipitate was collected and washed repeatedly with ethanol through centrifugal precipitation. Finally, precipitate was dried and

Received: October 7, 2013
Revised: March 16, 2014
Published: May 7, 2014

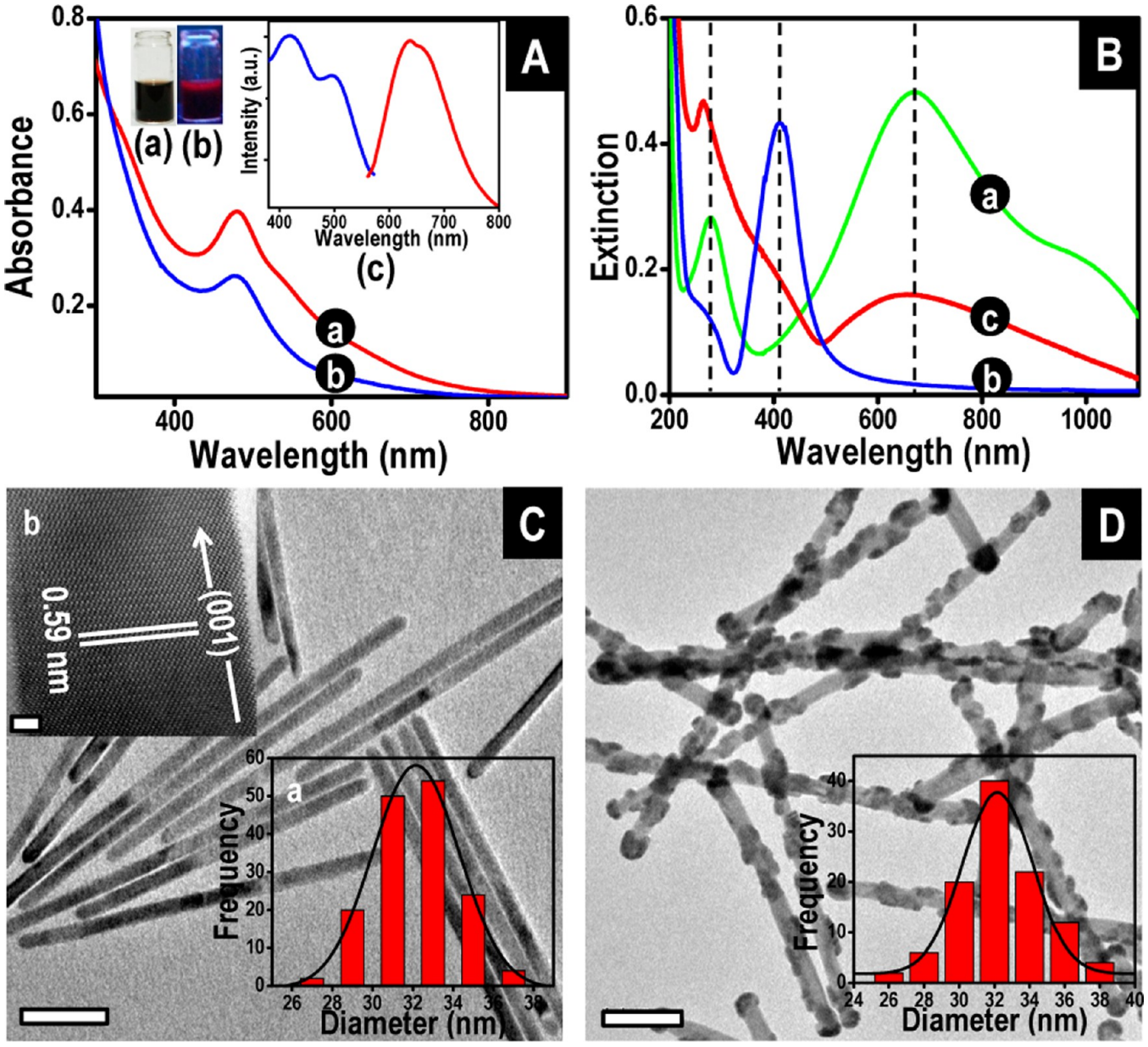

Figure 1. (A) UV−visible absorption spectra of as prepared (crude) [trace a] and gel separated [trace b] Ag_{32} cluster. Photographs of the solution of crude cluster under visible and UV light are shown in inset (a) and (b), respectively. The red emission is clearly visible only at the top as the UV excitation coming from the top attenuates with depth. Excitation and emission spectra of the crude cluster are shown in inset (c). (B) The UV−visible extinction spectrum of Te NWs reacted with Ag cluster (trace c) is shown along with the spectra of Te NWs (trace a) and citrate capped Ag NPs (trace b). Emergence of a new peak in the spectrum around 400 nm indicates the formation of Ag NPs. (C) The TEM image of parent Te NWs, diameter distribution of the NWs is shown in the inset a. A high resolution TEM image of a Te NW is shown in inset b. (D) The TEM image of NWs decorated with nodules obtained through Ag cluster reaction with Te NW. Diameter distribution of the nodule-free regions of the NWs is shown in the inset. Scale bar in the TEM images (C) and (D) is 100 nm and is 2 nm for the inset of (C).

collected as a reddish brown powder (~26 mg). This was termed as crude cluster (CC) in this paper.

Synthesis of Te NWs. Te NWs were prepared by the chemical method; originally reported by Chang et al.[28] In a typical procedure, 24 mg of TeO_2 powder was slowly added to a beaker containing 10 mL of hydrazine monohydrate. The reaction was allowed to continue at room temperature under constant magnetic stirring. The powder dissolved completely, and the color of the solution changed from colorless to blue indicating formation of Te NWs. After 1 h, the solution was diluted 10-fold with 10 mM SDS, in order to control the length of the NWs. The as-prepared solution was purified by centrifugation at 8000 rpm for 10 min. The residue was redispersed in deionized water. Centrifugation-redispersion cycle was repeated twice to remove any unreacted species and excess surfactant.

Synthesis of Ag NPs. Citrate capped Ag NPs were synthesized according to the Turkevich method.[43] 2 mL of 1 wt % trisodium citrate solution was added to a boiling 50 mL silver nitrate (1 mM) solution, and heating was continued further for a few minutes. The solution turned light yellow in color, indicating the formation of NPs. The suspension was cooled in an ice bath to allow the growth of NPs.

Glutathione capped Ag NPs were synthesized following the Creighton method of Ag colloid synthesis. Twelve mg of $NaBH_4$ was added to 100 mL of 0.1 mM solution of $AgNO_3$ under vigorous magnetic stirring at room temperature. To this yellow colored solution 2 mL of 1 mM glutathione (GSH) solution was added dropwise, and

dx.doi.org/10.1021/cm403288w | Chem. Mater. 2014, 26, 3049−3056

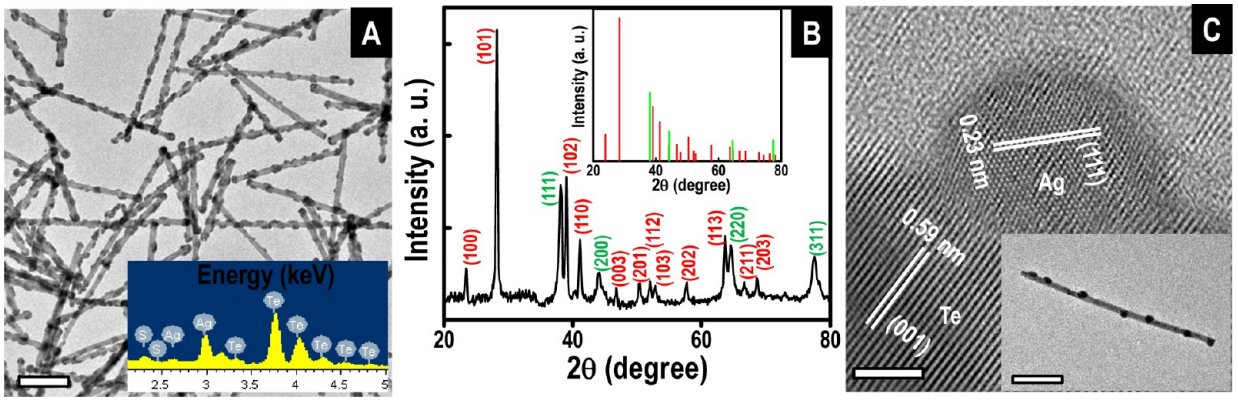

Figure 2. (A) A large area TEM image of nodule decorated NWs. The EDS spectrum taken from the same area is shown in the inset which shows the presence of both Ag and Te. Scale bar in the image is 200 nm. (B) XRD patterns of decorated Te NWs. All peaks are indexed to Ag (indexed in green) and Te (indexed in red). Standard peaks of Ag (JCPDS: 04-0783) and Te (JCPDS: 36-1452) are shown as stick patterns in the inset which match with the observed XRD pattern. (C) The HRTEM image of the decorated NWs showing crystalline nature of both the NW and the nodule. While the NW shows the Te phase, nodules are made up of Ag. A low magnification image of the corresponding NW is shown in the inset. Scale bar in the HRTEM is 5 nm and is 100 nm for the inset image. Characteristic planes of Te (001) and Ag (111) are marked.

stirring was continued for another 2 h in the dark to obtain stable colloidal Ag NPs.

Both citrate and glutathione capped Ag NPs were cleaned by centrifugal precipitation followed by redispersion in distilled water prior to reaction with Te NWs to ensure the removal of excess capping agent.

Reaction between Ag_{32} QC and Te NWs. Five mL of cleaned Te NW dispersion was mixed with different volumes of Ag_{32} QC solution (1 mg mL^{-1}) under constant magnetic stirring at room temperature, and the reaction was monitored with UV−visible spectroscopy at regular intervals until the completion of the reaction. Then the resulting dispersion was centrifuged at 7500 rpm for 10 min to precipitate the NWs. These NWs were then redispersed in distilled water and used for TEM analysis.

For solution phase heating experiments, an Eyela organic synthesizer was used to ensure uniform heating. The dispersion containing NWs after reaction with Ag QCs was maintained at various temperatures for different durations. Then the dispersion was centrifuged, redispersed, and spotted for TEM analysis. Structure of NWs was assessed from these images, and structural changes upon heating were identified.

■ INSTRUMENTATION

UV−visible absorption spectra were recorded using a PerkinElmer Lambda 25 spectrophotometer in the range 200−1100 nm. High-resolution transmission electron microscopy (HRTEM) was performed with a JEOL 3010, 300 kV instrument equipped with a UHR polepiece. Energy dispersive X-ray analysis (EDS) was carried out with an Oxford EDAX housed in the TEM. Samples were prepared by dropping the dispersion on carbon coated copper grids and drying in ambient condition. X-ray diffraction (XRD) data were collected with a Bruker AXS, D8 Discover diffractometer using Cu K_α (λ = 1.54 Å) radiation. Samples were scanned in the 2θ range from 10 to 90°. All the peaks were assigned and compared with the database published by the Joint Committee on Powder Diffraction Standards (JCPDS).

■ RESULTS AND DISCUSSION

Formation of Ag NPs Decorated Te NWs. Quantum clusters, being molecular in nature, exhibit molecule-like absorption features. Position and shape of these absorption bands depend on the size of the metal core.[8] For this reason, one cluster of a given atomicity can be distinguished from another by looking at their UV−visible absorption spectrum. A solid state method, developed originally for Ag_9 clusters,[44] was utilized for the synthesis of glutathione protected Ag_{32} clusters,[41] which was used in the studies reported here. The main reason to select Ag_{32} as the model Ag cluster for this study lies in its solubility in water. Although MSA (mercaptosuccinic acid) and MBA (mercaptobenzoic acid) protected Ag clusters are also water-soluble, they were not chosen to avoid possible structural deformation to the Te NWs induced by the ligands.[45] Another possible choice was Ag_{75} protected with SG,[46] but it is synthesized by formic acid reduction and when added to Te NWs dispersion, pH of the solution changes drastically and NWs tend to aggregate. As there are no other water-soluble clusters known, a comparative study of clusters has to wait some time. The effect of GSH on Te NWs was also investigated. Crystallinity of Te NWs was unaffected by GSH upon exposure for 24 h at room temperature. No other changes were seen in TEM.

As the characterization of Ag_{32} has been discussed earlier, we discuss only the essential aspects. The synthesis resulted in a brown colored, water-soluble solid, namely crude cluster (CC). The UV−visible spectrum (trace a, Figure 1A) of this brown solution (inset a, Figure 1A) shows a peak at 480 nm, accompanied by two shoulders at 350 and 550 nm. The characteristic feature of plasmonic Ag NPs was absent. The solution is red luminescent as can be seen from the photograph under UV light irradiation (inset b, Figure 1A) and also from the photoluminescence spectrum shown in inset c, Figure 1A. Further analysis with polyacrylamide gel electrophoresis (PAGE) proved that the crude cluster is a mixture of five different Ag@GSH clusters, with $Ag_{32}SG_{19}$ being the principal component. The UV−visible spectrum of gel separated $Ag_{32}SG_{19}$ (trace b) is shown in Figure 1A for comparison. As the crude cluster is by and large composed of Ag_{32}, for all the studies carried out in this paper, we used this sample.

Te NWs show two distinct interband transitions in their UV−visible extinction spectrum. Peak I originates from electronic transitions from p-bonding valence band (VB2) to p-antibonding conduction band (CB1) and appears in the range of 250−350 nm, whereas Peak II is due to the transition from p-lone pair valence band (VB3) to the p-antibonding conduction band (CB1) and appears around 600−850 nm.[28] In

dx.doi.org/10.1021/cm403288w | Chem. Mater. 2014, 26, 3049−3056

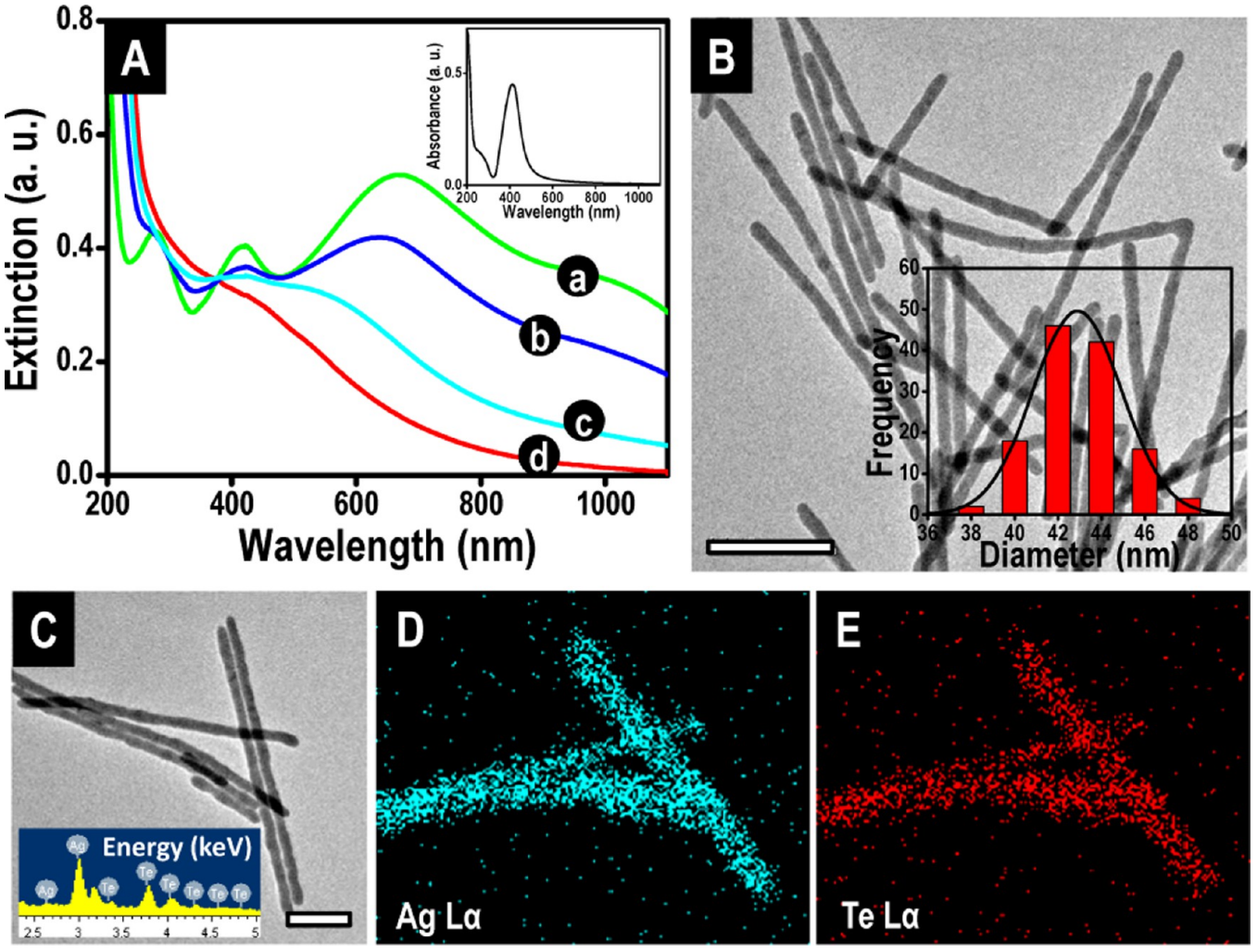

Figure 3. (A) Time dependent UV−visible extinction spectra of a solution containing Ag NPs and Te NWs. Traces a, b, c, and d represent the spectrum after 0, 6, 12, and 24 h, respectively. The spectrum of citrate capped Ag NPs is shown in the inset. (B) The TEM image of the NWs formed after 24 h. Diameter distribution of the NWs is shown in the inset. (C) The TEM image and the EDS spectrum of the NWs. EDS intensity map for Ag (D) and Te (E) for the same area are shown. Scale bar is 200 nm in (B) and 100 nm in (C).

our synthesis, the positions of these peaks were 280 and 680 nm, respectively (trace a, Figure 1B). The spectrum of Te NWs after reaction with Ag_{32} QCs is shown in trace b, and it shows a small hump around 400 nm where the surface plasmon resonance (SPR) peak of Ag NPs appears (trace c). The two peaks characteristic to Te NWs remain, albeit a slight shift in their positions and intensities was observed. A similar trend was observed for the growth of Au NP on Te NWs,[47] though the Au plasmon peak was found to appear only at a very high concentration of Au NPs. The presence of the 400 nm band in the spectrum possibly results from higher surface electron density in Ag than Au, which gives rise to a better plasmonic property in Ag.[48] A representative TEM image of the parent Te NWs is shown in Figure 1C. The HRTEM image of the Te NW (inset b) shows the (001) directed anisotropic growth in it. Diameter distribution of these NWs (inset a) was obtained by measuring diameters of NWs from several TEM images. Parent Te NWs had an average diameter of 32 nm. Reaction of Te NWs with Ag_{32} QC leads to the formation of nodular growth at different locations of the NW. A TEM image of such NWs is shown in Figure 1D. Diameter distribution of regions without such growth is shown in the inset of the image, and average diameter of those regions is the same as that of the parent NWs. From these analyses, we presumed the resulting products to be Ag−Te hybrid NWs.

Structural characterization of the NWs having nodular growth was performed using spectroscopy, diffraction, and microscopy. A large area TEM image of the NWs with nodular growth on them is shown in Figure 2A. The EDS spectrum taken from the same area is shown in the inset of the figure and the presence of both Ag and Te can be seen. The XRD pattern of these NWs is presented in Figure 2B. The combined JCPDS pattern for hexagonal Te (JCPDS: 36-1452) and cubic Ag phase (JCPDS: 04-0783) is shown in the inset, and it resembles the observed pattern. Final structural conformation of the NW structures came from the analyses of the HRTEM image presented in Figure 2C. The nodular growth was identified to be due to Ag, while Te NW retained its original (001) oriented hexagonal structure. A low magnification TEM image of the same NW is shown in the inset.

Difference in Reactivity of Silver Cluster Compared to Ag^+ and Ag Nanoparticle. Reactivity of Ag_{32} QCs with Te NWs in solution is in stark contrast with that of Ag^+. With the addition of Ag^+, blue colored Te NWs dispersion convert to brown colored Ag_2Te NWs dispersion almost instantaneously.[30] This transformation is reflected in the UV−visible

dx.doi.org/10.1021/cm403288w | *Chem. Mater.* 2014, 26, 3049−3056

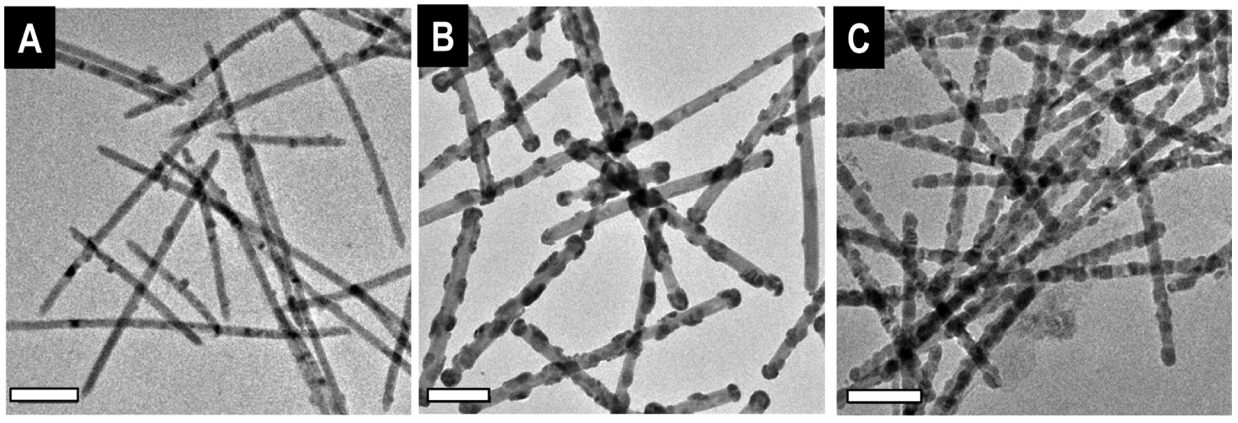

Figure 4. Increase in the extent of nodule coverage of the NWs with increasing amount of Ag_{32} QCs added: (A) 200 μL, (B) 1 mL, and (C) 2 mL. Scale bar in the images is 100 nm.

spectra of the NWs (Supporting Information, SI, Figure S1A), where peaks due to Te NWs (trace a) diminish with the emergence of a broad band around 480 nm (trace b). Reactivity of Te NWs with another Ag(0) nanosystem, namely Ag NPs (citrate capped), was also investigated. The TEM image of the citrate capped Ag NPs used for this study is shown in Figure S1B. They were found to form the same end product of Ag_2Te NWs. UV−visible spectra of a mixture of Te NWs and Ag NPs after 0, 6, 12, and 24 h (traces a, b, c and d, respectively) are shown in Figure 3A. Peaks due to both Ag NPs and Te NWs diminished over time, and the spectrum of the solution after 24 h (trace d) appeared exactly similar to that of Ag_2Te NWs. The TEM image taken from the solution after 24 h of reaction showed the presence of only NWs. These NWs were 33% larger in diameter (inset, Figure 3B) and 15% longer (Figure S2) than the parent Te NWs, and this matches with the reported volume change for Te to Ag_2Te conversion.[32] The EDS spectrum of the formed NWs (inset, Figure 3C) showed the presence of Ag and Te in a 2:1 atomic ratio, and equal distribution of these elements throughout the NWs (Figure 3D and E, respectively) confirmed NWs composition to be Ag_2Te. XRD and HRTEM (Figure S2) of the NWs further established their identity.

This similar but slow reactivity of Ag NPs compared to Ag^+ can be explained by the slow Ag^+ leaching property of Ag NPs. Ag NPs are known to release Ag^+ in water,[49] which react with the Te NWs present in the solution. Consumption of the released Ag^+ by reaction enhances the leaching, and all the Ag NPs present slowly get consumed. Te NWs transform into Ag_2Te NWs in due course, but Ag_{32} QCs, being highly capped with strong thiolate ligands, do not release Ag^+ into the solution and silver telluride does not form.

We probed the reactivity of GSH capped Ag NPs also with Te NWs to understand the difference in reactivity between particles of two different size regimes but with the same capping agent. However, GSH capped Ag NPs did not attach themselves to the Te NWs to form a hybrid Ag−Te nanostructure, nor did they form Ag_2Te NWs by reacting with Te NWs at room temperature, even after 24 h. Te NWs and GSH capped Ag NPs remained as separated entities in solution (Figure S3).

Probable Mechanism of Ag Nodule Decorated Te NW Formation. With decrease in size of a metal particle, the population of atoms with reduced coordination number increases, resulting in the increase in surface free energy of the particle. This induces a tendency toward aggregation in small clusters. These small clusters, when put on a surface, tend to diffuse across the surface and during this movement, as one cluster encounters another; they coalesce to form bigger particles.[50−52] In the case of monolayer protected Ag clusters, although the core silver atoms are protected by a monolayer of thiolates, this protection is incomplete, and certain core atoms are still accessible as evident from the formation of alloy clusters.[26] Due to this incomplete protection from thiolate, these clusters have an inherent tendency to coalesce to form nanoparticles. This process of coalescence does not happen in solution as SG groups carry charge, and so the clusters repel each other; but when put on surfaces, charge neutralization can happen, and the clusters can come together through diffusion and form bigger NPs. In our experiment, Ag_{32} clusters coalesce on the surface of Te NWs when put together in solution, and they form Ag islands on the NW surface.

This phenomenon, being diffusion controlled, leads to the formation of polydispersed particles on the surfaces. Again, for the same reason, particles do not grow beyond a certain size. To check the validity of the conjecture of NP formation by diffusion-controlled aggregation of Ag_{32} QCs on the Te NW surface, different volumes of the QC solution were reacted with the same amount of Te NW dispersion. As 200 μL of QC solution was reacted, formation of very few small sized nodules on Te NWs was observed (Figure 4A). When the volume of QC solution was increased to 1 mL, the number of nodules formed per NW increased and so did their size (Figure 4B); but as the amount of cluster was further increased to 2 mL, though the number of nodules and their coverage increased, the size of the formed nodules remained nearly the same (Figure 4C). Size distribution of the nodules formed in 1 and 2 mL cases is shown in Figure S4. UV−visible spectra for all these three NWs are shown in Figure S5A. The NWs obtained by 2 mL of QC addition are almost completely covered with Ag nodules, and with further addition of QC, no change in the UV−visible spectrum was observed.

Change in Nanowire Morphology upon Heating. The morphology of these Ag-nodule decorated Te NWs was found to be very sensitive to the temperature of the solution. Figure 5 shows morphology evolution of the NWs as the NWs dispersion was maintained at 60 °C. The shape evolution was checked by collecting the NWs by centrifugal precipitation from the heated solution and subjecting them to TEM analysis at different time intervals. Figure 5A shows the TEM image of

dx.doi.org/10.1021/cm403288w | *Chem. Mater.* 2014, 26, 3049−3056

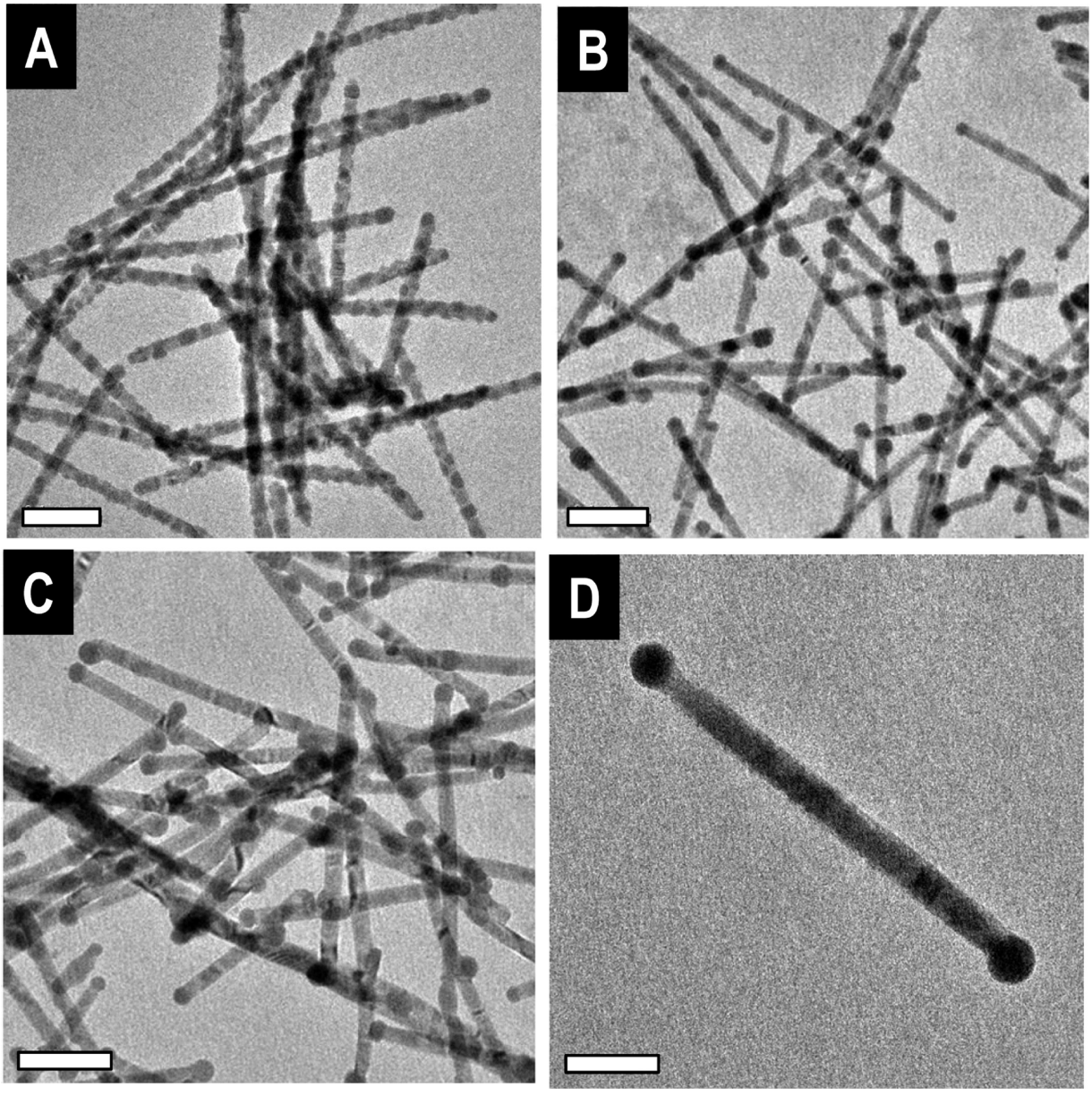

Figure 5. Effect of solution phase heating on the morphology of the Ag nodule-decorated Te NWs. (A) The TEM image of the parent decorated NWs. (B) After 3 h of heating, nodules are bigger in size and occur only at the two ends and very few on the NW sidewalls. (C) After 6 h of heating, bigger nodules are present toward the NW ends and these resemble dumbbells. (D) The TEM image of a single dumbbell-shaped NW. Scale bar in (A)-(C) is 100 nm, and it is 50 nm in (D).

the NWs before heating. On solution phase heating, aggregation and movement of the nodules toward the tips of the NWs were observed. In Figure 5B, a TEM image of the NWs after 3 h of heating is presented. These NWs have a few big nodules present on their side walls with almost all of them having two big nodules present at the tips. After 6 h of heating, nodules present on the NW side walls vanish, and the resulting NWs morphology resembles that of a nano dumbbell in which two big sphere-shaped particles are joined by a NW section (Figure 5C). The TEM image of a single nano dumbbell is given in Figure 5D. At this point, we would also like to stretch that this morphological evolution in the nodule decorated NWs was observed only at a higher solution temperature. Keeping the as-prepared NWs in solution at room temperature did not bring out such morphological changes in them.

Structural identification of these nano dumbbells was performed with EDS and HRTEM. Ag and Te EDS intensity maps of such a NW were combined and that is shown in Figure 6A. Te was found only in the middle section, whereas the ball-shaped structures had only Ag in them. This kind of Ag−Te−Ag structure of the nano dumbbells was also confirmed from the HRTEM image of one end of a nano dumbbell (Figure 6B), where the presence of Ag in the end segment and Te in the middle can be observed. The XRD pattern of these NWs is given in Figure S5B, and coexistence of both Ag and Te phases in them can be observed.

Growth of Au NPs is traditionally employed for the identification of high energy and defect sites in nanostructures.[53,54] In Te NWs, due to their unique *c*-axis oriented growth, the (001) planes are present at both ends, whereas the sidewalls are composed of (110) and its centrosymmetric

dx.doi.org/10.1021/cm403288w | *Chem. Mater.* 2014, 26, 3049−3056

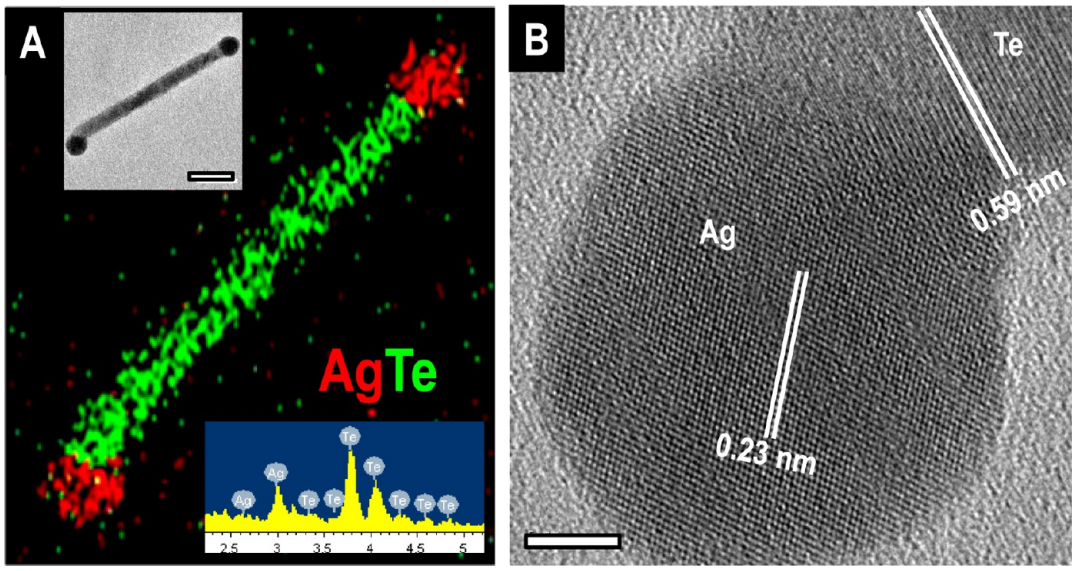

Figure 6. (A) Overlaid Ag and Te EDS intensity maps showing the distribution of Te and Ag in the dumbbell-shaped NW. While Te is the component of the NWs, the ball-shaped ends are composed of Ag. The corresponding TEM image and the EDS spectrum are given in the insets. Scale bar in the TEM image is 50 nm. (B) The HRTEM image of the dumbbell-shaped NWs showing the presence of Ag at the ends and Te in the middle. Scale bar is 5 nm.

planes. Surface energy of (001) plane is higher than that of (110).[55] Due to this reason, the ends are more reactive than the body which was revealed in the growth of Au NPs on Te NWs.[56] In the present case, the presence of the Ag caps on the tips of Te NWs reduces the overall surface energy of the NWs. The presence of two bigger NPs also decreases the surface energy of Ag system than the presence of several small Ag nodules, and this overall minimization of surface energy in a dumbbell structure leads to the transformation observed at elevated temperature.

This process of Ag−Te−Ag nano dumbbell formation from the Ag nodule-decorated Te NWs was found to be sensitive to the solution temperature. When the temperature was maintained at 80 °C, silver was found to diffuse within Te lattice forming silver incorporated NWs (Figure S6). While the exact nature of the transformation of nodule decorated NWs into dumbbell-shaped NWs is not fully understood, this may be seen as a "nanoscale zone refining" process. The bigger nodules acquire sufficient energy to become mobile on the NW surface[51] at high solution temperature (60 °C), coalesce with each other, and move toward the tips; but, at even higher temperature (80 °C), Ag atoms in the nodules gain enough energy to diffuse into the Te lattice. The nature of solution also plays an important role in this process. As we analyzed the mother liquor with electrospray ionization (ESI) mass spectrometry, the presence of glutathione (as Na salt) and its dimer was found in the solution (Figure S7). These species probably originate during the cluster coalescence where excess ligand is thrown into the solution. We presume that these species play an important role in the stabilization of the Ag nodules. As the mother liquor was discarded through centrifugation and decorated NWs were redispersed in distilled water, propensity of silver diffusion into Te increases, and the incorporation of Ag into Te lattice happens at 60 °C (Figure S8).

We checked the fate of the mixture of GSH capped Ag NPs and Te NWs solution at elevated temperature as ligand binding of SG to the NP surface is expected to weaken at higher temperature and that may lead to reaction with Te NWs; but even at 60 °C, we did not observe any reaction between the two species, while at 80 °C they slowly (over a period of 40 h) react with each other to give Ag_2Te NWs.

SUMMARY AND CONCLUSIONS

In summary, we probed the unique chemistry of a glutathione protected, water-soluble Ag QC upon its interaction with a 1D nanosystem, Te NWs. The QC reactivity was found to be quite different than that of silver ions as well as Ag NPs. Clusters coalesce on the NW surface to form NPs. This leads to the formation of a new material, Ag nodule-decorated Te NWs. A controlled solution phase heating of this material brings about changes in the morphology, and dumbbell-shaped Ag−Te−Ag NWs are formed. Both of these new materials (nodule decorated Te NWs and double dumbbell Ag−Te−Ag NWs) can have potential applications in the fabrication of electronic devices. The study suggests an unusual difference in the reactivity of nanosystems leading to the formation of novel structures. Although the formation of such structures may be reasoned, an accurate molecular understanding requires additional efforts.

ASSOCIATED CONTENT

Supporting Information

UV−visible spectra of Te and Ag_2Te NWs, TEM images of Ag NPs, length distribution of Te and Ag_2Te NWs, HRTEM and XRD of Ag_2Te NWs, TEM and HRTEM images of a mixture of Te NW and GSH capped Ag NP after 24 h of reaction, diameter distribution of the nodules formed with the addition of 1 and 2 mL of cluster solution, UV−visible spectra of Ag nodule decorated NWs for different cluster concentrations, XRD of dumbbell-shaped Ag−Te−Ag NWs, TEM and EDS of NWs heated at 80 °C, the ESI mass spectrum of the mother liquor, TEM and EDS of NWs heated at 60 °C after removal of mother liquor and redispersion in distilled water. This material is available free of charge via the Internet at http://pubs.acs.org

dx.doi.org/10.1021/cm403288w | *Chem. Mater.* 2014, 26, 3049−3056

AUTHOR INFORMATION

Corresponding Author

*E-mail: pradeep@iitm.ac.in.

Author Contributions

‡These authors contributed equally.

Notes

The authors declare no competing financial interest.

ACKNOWLEDGMENTS

We thank the Department of Science and Technology, Government of India for constantly supporting our research program on nanomaterials. A.S. and M.S.B. thank CSIR, Govt. of India for research fellowships.

REFERENCES

(1) Sajanlal, P. R.; Sreeprasad, T. S.; Samal, A. K.; Pradeep, T. *Nano Rev.* **2011**, DOI: doi: 10.3402/nano.v2i0.5883.

(2) Shibu, E. S.; Pradeep, T. *Chem. Mater.* **2011**, *23*, 989.

(3) Adhikari, B.; Banerjee, A. *Chem. Mater.* **2010**, *22*, 4364.

(4) Harkness, K. M.; Tang, Y.; Dass, A.; Pan, J.; Kothalawala, N.; Reddy, V. J.; Cliffel, D. E.; Demeler, B.; Stellacci, F.; Bakr, O. M.; McLean, J. A. *Nanoscale* **2012**, *4*, 4269.

(5) Nimmala, P. R.; Dass, A. *J. Am. Chem. Soc.* **2011**, *133*, 9175.

(6) Qian, H.; Zhu, M.; Wu, Z.; Jin, R. *Acc. Chem. Res.* **2012**, *45*, 1470.

(7) Jin, R. *Nanoscale* **2010**, *2*, 343.

(8) Udayabhaskararao, T.; Pradeep, T. *J. Phys. Chem. Lett.* **2013**, *4*, 1553.

(9) Diez, I.; Ras, R. H. A. *Nanoscale* **2011**, *3*, 1963.

(10) Lu, Y.; Chen, W. *Chem. Soc. Rev.* **2012**, *41*, 3594.

(11) Diez, I.; Kanyuk, M. I.; Demchenko, A. P.; Walther, A.; Jiang, H.; Ikkala, O.; Ras, R. H. A. *Nanoscale* **2012**, *4*, 4434.

(12) Chakraborty, I.; Govindarajan, A.; Erusappan, J.; Ghosh, A.; Pradeep, T.; Yoon, B.; Whetten, R. L.; Landman, U. *Nano Lett.* **2012**, *12*, 5861.

(13) Abdul, H. L. G.; Ashraf, S.; Katsiev, K.; Kirmani, A. R.; Kothalawala, N.; Anjum, D. H.; Abbas, S.; Amassian, A.; Stellacci, F.; Dass, A.; Hussain, I.; Bakr, O. M. *J. Mater. Chem. A* **2013**, *1*, 10148.

(14) Rao, T. U. B.; Pradeep, T. *Angew. Chem., Int. Ed.* **2010**, *49*, 3925.

(15) Dhanalakshmi, L.; Udayabhaskararao, T.; Pradeep, T. *Chem. Commun.* **2012**, *48*, 859.

(16) Wu, Z.; Lanni, E.; Chen, W.; Bier, M. E.; Ly, D.; Jin, R. *J. Am. Chem. Soc.* **2009**, *131*, 16672.

(17) Yang, H.; Wang, Y.; Zheng, N. *Nanoscale* **2013**, *5*, 2674.

(18) Desireddy, A.; Conn, B. E.; Guo, J.; Yoon, B.; Barnett, R. N.; Monahan, B. M.; Kirschbaum, K.; Griffith, W. P.; Whetten, R. L.; Landman, U.; Bigioni, T. P. *Nature* **2013**, *501*, 399.

(19) Yang, H.; Wang, Y.; Huang, H.; Gell, L.; Lehtovaara, L.; Malola, S.; Hakkinen, H.; Zheng, N. *Nat. Commun.* **2013**, *4*, 3422.

(20) Nishida, N.; Yao, H.; Ueda, T.; Sasaki, A.; Kimura, K. *Chem. Mater.* **2007**, *19*, 2831.

(21) Chakraborty, I.; Bag, S.; Landman, U.; Pradeep, T. *J. Phys. Chem. Lett.* **2013**, *4*, 2769.

(22) Zhu, M.; Chan, G.; Qian, H.; Jin, R. *Nanoscale* **2011**, *3*, 1703.

(23) Bootharaju, M. S.; Deepesh, G. K.; Udayabhaskararao, T.; Pradeep, T. *J. Mater. Chem. A* **2013**, *1*, 611.

(24) Cathcart, N.; Kitaev, V. *ACS Nano* **2011**, *5*, 7411.

(25) Cathcart, N.; Kitaev, V. *Nanoscale* **2012**, *4*, 6981.

(26) Udayabhaskararao, T.; Sun, Y.; Goswami, N.; Pal, S. K.; Balasubramanian, K.; Pradeep, T. *Angew. Chem., Int. Ed.* **2012**, *51*, 2155.

(27) Chakraborty, I.; Udayabhaskararao, T.; Pradeep, T. *J. Hazard. Mater.* **2012**, *211−212*, 396.

(28) Lin, Z.-H.; Yang, Z.; Chang, H.-T. *Cryst. Growth Des.* **2008**, *8*, 351.

(29) Liu, Z.; Hu, Z.; Liang, J.; Li, S.; Yang, Y.; Peng, S.; Qian, Y. *Langmuir* **2004**, *20*, 214.

(30) Samal, A. K.; Pradeep, T. *J. Phys. Chem. C* **2009**, *113*, 13539.

(31) Samal, A. K.; Pradeep, T. *J. Phys. Chem. C* **2010**, *114*, 5871.

(32) Moon, G. D.; Ko, S.; Xia, Y.; Jeong, U. *ACS Nano* **2010**, *4*, 2307.

(33) Liang, H.-W.; Liu, S.; Yu, S.-H. *Adv. Mater.* **2010**, *22*, 3925.

(34) Wang, W.-S.; Goebl, J.; He, L.; Aloni, S.; Hu, Y.-X.; Zhen, L.; Yin, Y.-D. *J. Am. Chem. Soc.* **2010**, *132*, 17316.

(35) Samal, A. K.; Pradeep, T. *Nanoscale* **2011**, *3*, 4840.

(36) Som, A.; Pradeep, T. *Nanoscale* **2012**, *4*, 4537.

(37) Zhang, G.; Fang, H.; Yang, H.; Jauregui, L. A.; Chen, Y. P.; Wu, Y. *Nano Lett.* **2012**, *12*, 3627.

(38) Liu, J.-W.; Huang, W.-R.; Gong, M.; Zhang, M.; Wang, J.-L.; Zheng, J.; Yu, S.-H. *Adv. Mater.* **2013**, *25*, 5910.

(39) Liu, J.-W.; Xu, J.; Liang, H.-W.; Wang, K.; Yu, S.-H. *Angew. Chem., Int. Ed.* **2012**, *51*, 7420.

(40) Liang, H.-W.; Liu, J.-W.; Qian, H.-S.; Yu, S.-H. *Acc. Chem. Res.* **2013**, *46*, 1450.

(41) Udayabhaskararao, T.; Bootharaju, M. S.; Pradeep, T. *Nanoscale* **2013**, *5*, 9404.

(42) Guo, J.; Kumar, S.; Bolan, M.; Desireddy, A.; Bigioni, T. P.; Griffith, W. P. *Anal. Chem.* **2012**, *84*, 5304.

(43) Pillai, Z. S.; Kamat, P. V. *J. Phys. Chem. B* **2004**, *108*, 945.

(44) Rao, T. U. B.; Nataraju, B.; Pradeep, T. *J. Am. Chem. Soc.* **2010**, *132*, 16304.

(45) Sreeprasad, T. S.; Samal, A. K.; Pradeep, T. *Chem. Mater.* **2009**, *21*, 4527.

(46) Chakraborty, I.; Udayabhaskararao, T.; Pradeep, T. *Chem. Commun.* **2012**, *48*, 6788.

(47) Lin, Z.-H.; Chang, H.-T. *Langmuir* **2008**, *24*, 365.

(48) Amendola, V.; Bakr, O. M.; Stellacci, F. *Plasmonics* **2010**, *5*, 85.

(49) Sankar, M. U.; Aigal, S.; Maliyekkal, S. M.; Chaudhary, A.; Anshup; Kumar, A. A.; Chaudhari, K.; Pradeep, T. *Proc. Natl. Acad. Sci. U. S. A.* **2013**, *110*, 8459.

(50) Bardotti, L.; Jensen, P.; Hoareau, A.; Treilleux, M.; Cabaud, B. *Phys. Rev. Lett.* **1995**, *74*, 4694.

(51) Goldby, I. M.; Kuipers, L.; von Issendorff, B.; Palmer, R. E. *Appl. Phys. Lett.* **1996**, *69*, 2819.

(52) Ye, G.-X.; Michely, T.; Weidenhof, V.; Friedrich, I.; Wuttig, M. *Phys. Rev. Lett.* **1998**, *81*, 622.

(53) Mokari, T.; Rothenberg, E.; Popov, I.; Costi, R.; Banin, U. *Science* **2004**, *304*, 1787.

(54) Liu, Y.-H.; Wayman, V. L.; Gibbons, P. C.; Loomis, R. A.; Buhro, W. E. *Nano Lett.* **2010**, *10*, 352.

(55) Li, Z.; Zheng, S.; Zhang, Y.; Teng, R.; Huang, T.; Chen, C.; Lu, G. *J. Mater. Chem. A* **2013**, *1*, 15046.

(56) Lin, Z.-H.; Lin, Y.-W.; Lee, K.-H.; Chang, H.-T. *J. Mater. Chem.* **2008**, *18*, 2569.